Feedback stimulation strategy: control of retinal ganglion cells activation

Tatiana Kameneva[1,*], David B. Grayden[1,2,3], Hamish Meffin[1,3], Anthony N. Burkitt[1,2,3]

***Abstract*— It is possible to cause a sensation of light in patients who have lost photoreceptors due to degenerative eye diseases by targeting surviving neurons with electrical stimulation by means of visual prosthetic devices. All stimulation strategies in currently used visual prostheses are open-loop, that is, the stimulation parameters do not depend on the level of activation of neurons surrounding stimulating electrodes. In this paper, we investigate a closed-loop stimulation strategy using computer simulations of previously constrained models of ON and OFF retinal ganglion cells. Using a proportional-integral-type controller we show that it is possible to control activation level of both types of retinal ganglion cells. We also demonstrate that the controller tuned for a particular combination of synaptic currents continues to work during retina degeneration when excitatory currents are reduced by 20%.**

I. INTRODUCTION

In patients who have degenerative eye diseases such as retinitis pigmentosa and age-related macular degeneration a substantial fraction of retinal ganglion cells (RGCs) survive photoreceptor loss [6]. By targeting surviving neurons with electrical stimulation, a number of research groups have been able to restore rudimentary vision to patients implanted with a visual prostheses [1]. The patients perceive spots of light called "phosphenes". A mosaic of phosphenes with different size and brightness may code a black-and-white two-dimensional image.

Currently used stimulation strategies in visual prostheses are open-loop, that is, the stimulation level is fitted to each patient interactively based on the patient's reported perception in the clinic and do not rely on any measure of the response of neural tissue in the proximity of the implanted electrode array. We propose to use a closed-loop technique to adjust stimulation parameters dynamically online based on the response of retinal neurons. This technique has many advantages, including a possibility to reduce power consumption, to address variability in performance between patients, and to activate different types of cells selectively or simultaneously. In this work, we consider activation of two types of ganglion cells: ON and OFF RGCs.

ON and OFF RGCs display differences in their intrinsic electrophysiology. In the absence of any input, OFF cells maintain spontaneous activity, exhibit rebound excitation, burst firing, and subthreshold membrane potential oscillations. ON cells do not spike in the absence of synaptic input, and display none of the aforementioned phenomena [7]. In the absence of sensory input, the resting spike activity of RGCs in normal retina is irregular. However, with retinal degeneration, the balance of inhibitory and excitatory input is different for ON and OFF RGCs, and a rhythmic synaptic input drives regular bursts of spikes in both ON and OFF cells at a frequency of around 10 Hz [8].

In this study, we use previously constrained models of ON and OFF RGCs based on published experimental data with and without synaptic blockers [7], [8]. Using Hodgkin-Huxley-type single compartment models, we investigate cells responses to electrical stimulation using a closed-loop paradigm. We propose to implement a proportional-integral-derivative-type (PID) controller to control activation of ganglion cells. PID controllers have become almost universally used in industrial control applications. Moreover, PID controllers have been used in the field of medical bionics to modulate seizures [10], to control the instantaneous response probability of cortical neurons [12], and to compensate for drift in a neuron's firing rate to constant synaptic input [9]. A PID controller is a generic design that minimizes the error between the output of a system and the reference signal by adjusting the input to the system.

II. METHODS

Intrinsic electrophysiology

The intrinsic electrophysiology of RGCs was modelled using Hodgkin-Huxley-like model by summing ionic currents using Kirchoff's law:

$$C_{\rm m}\frac{dV}{dt} = \bar{g}_{\rm L}(V-V_{\rm L})+\bar{g}_{\rm Na}m^3h(V-V_{\rm Na})+\bar{g}_{\rm Ca}c^3(V-V_{\rm Ca}) +(\bar{g}_{\rm K}n^4+\bar{g}_{\rm K,A}a^3h_{\rm A}+\bar{g}_{\rm K(Ca)})(V-V_{\rm K}) +\bar{g}_{\rm h}l(V-V_{\rm h})+\bar{g}_{\rm T}m_{\rm T}^3h_{\rm T}(V-V_{\rm T})+\bar{g}_{\rm NaP}p(V-V_{\rm Na})+I_{\rm stim}, \quad (1)$$

where V is the membrane potential, $C_{\rm m}$ is the specific capacitance of the membrane, $\bar{g}$ is the maximum conductance of an ionic current defined by the subscript, $I_{\rm stim}$ is an intracellular stimulation current. Leak, sodium, calcium, delayed rectifier potassium, A-type, and Ca-activated potassium currents had dynamics the same as in [2]. The hyperpolarization-activated, low-voltage-activated calcium, and sodium persistent currents were modelled as in [14], [13], [11]. The data from [7] was used to constraint the model. For details, see [4]. All parameters in simulations were set the same as in [4], with $\bar{g}_{\rm h}=4\times10^{-6}$ S/cm^2, $\bar{g}_{\rm NaP}=5\times10^{-8}$ S/cm^2, $\bar{g}_{\rm T}=0$ S/cm^2 for ON cells, and $\bar{g}_{\rm T}=6\times10^{-4}$ S/cm^2 for OFF cells.

The only reversal potential that was allowed to vary with time was $V_{\rm Ca}$. Gating variables $m, h, c, n, a, h_{\rm A}, l, m_{\rm T}, p$ of the voltage-gated currents were described by the first-order

[1] NeuroEngineering Laboratory, Department of Electrical Electronic Engineering, The University of Melbourne, Australia. [2] Bionics Institute, East Melbourne, Australia. [3] National ICT Australia, NICTA, Australia. *tkam@unimelb.edu.au

978-1-4244-7929-0/14/$26.00 ©2014 IEEE

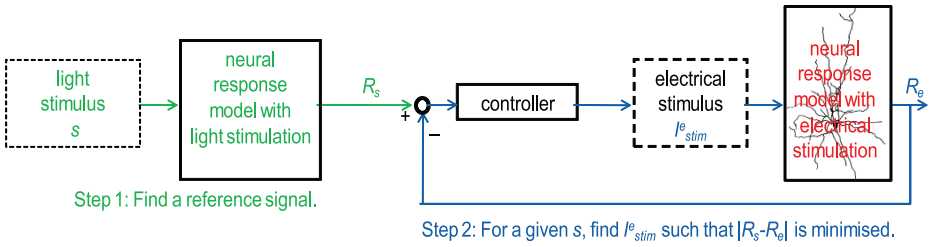

Fig. 1. Closed-loop stimulation diagram for a visual prosthesis. s is the light stimulus, $R_{\rm s}$ is the reference signal,$R_{\rm e}$ is the recorded spiking rate, $I^e_{\rm stim}$ is electrical stimulation level.

kinetic equations [2]. Computer simulations of RGC activity were performed in the NEURON environment using a single-compartment consisting of one segment, taken as a cylinder with diameter and length both 25 μm, which is similar to a ganglion cell soma. All voltage-dependent parameters were initialized at a membrane potential value of -65 mV.

The models of ON and OFF RGCs were constrained using experimental data from wild-type mice. It was shown that intrinsic properties of RGCs are maintained in mice with retinal degeneration [8].

Synaptic currents

The models of ON and OFF cells with added synaptic currents were constrained previously to reproduce maintained rhythmic spiking based on data in [8]: rhythmic bursts of spikes at 10 Hz frequency. For details, see [5]. The dynamics of the inhibitory and excitatory currents were described by:

$$I_{\rm inh} = g_{\rm inh}(t)(V - V_{\rm inh}), \qquad (2)$$

$$I_{\rm exc} = g_{\rm exc}(t)(V - V_{\rm exc}), \qquad (3)$$

where $g_{\rm inh}, g_{\rm exc}$ are the time-varying conductances; $V_{\rm inh} = -70$ mV, $V_{\rm exc} = 0$ mV are the reversal potentials for the inhibitory and excitatory currents. To model ON and OFF cells with synaptic currents, the terms (2), (3) were added to the right-hand side of (1). Note, the values in these terms are different for ON and OFF RGCs, see [5] for details.

Electrical stimulation

The constrained models of ON and OFF RGCs with and without synaptic currents were used to investigate responses of cells to electrical stimulation using a feedback paradigm. The feedback block-diagram for stimulation is shown in Fig. 1, where s is the light stimulus, $R_{\rm s}$ is the reference signal (a desired neural spike rate), $I^e_{\rm stim}$ is the level of electrical stimulation, and $R_{\rm e}$ is the recorded spiking rate. In this paper, we do not discuss Step 1, how the light stimulation was converted into a reference signal.

In the currently used visual implants, there are no means to stimulate neurons individually, but rather populations of cells are stimulated simultaneously. We assume that we can control the instantaneous spiking rate of the individual cells, $R_{\rm e}$, in response to the electrical stimulation, and that the extracellular stimulation, $I^e_{\rm stim}$, is proportional to the intracellularly injected current, $I_{\rm stim}$, in (1).

Given the membrane potential, V, in (1), the instantaneous spiking rate, $R_{\rm e}$, was calculated as the inverse of the inter-spike-interval between two consecutive spikes. The time of the spike was calculated as the time at which the membrane potential crossed the zero-threshold in a positive direction.

The classical form of the PID controller is the following:

$$I_{\rm stim}(t) = K_{\rm p}e(t) + K_{\rm i}\int_{t_1}^{t} e(x)dx + K_{\rm d}\frac{d}{dt}e(t), \qquad (4)$$

where $K_{\rm p}, K_{\rm i}$, and $K_{\rm d}$ are the proportional, integral, and derivative gains. In the context illustrated in Fig. 1 and given the assumptions, the error is the difference between the desired neural response, $R_{\rm s}$, and the actual neural response, $R_{\rm e}$, evoked by the stimulus, $I_{\rm stim}$; i.e., $e = R_{\rm s} - R_{\rm e}$. We used the spiking rate on the previous three inter-spike-intervals in order to calculate the integral term on the controller. Here, the integral in (4) was calculated using three previous inter-spike-intervals, $t_1 = t - 3$.

Similar to [9], we assumed that the derivative term is zero due to high variability between spikes. To find the proportional and integral gains two techniques were used: Ziegler-Nichols method and manual tuning. The Ziegler-Nichols method involved two steps in response to the step reference (25 Hz step, 500 ms delay, 8000 ms duration). First, $K_{\rm i}$ was set to zero and $K_{\rm p}$ was increased until it reached a value $K_{\rm u}$, at which the output of the system started to oscillate. The values of $K_{\rm u}$ and the oscillation period, $P_{\rm u}$, were used to set the gains as follows: $K_{\rm p} = 0.45K_{\rm u}$, $K_{\rm i} = 1.2K_{\rm p}/P_{\rm u}$. Due to very strong intrinsic 10-Hz oscillations in RGCs with synaptic currents, it was impossible to detect oscillations due to applied stimulation. Therefore, for the RGCs with synaptic currents, manual tuning was only used to set the gains of the controller.

We also explored two types of proportional-integral controller, in which the amplitude of the stimulation was decreased proportional to the accumulative spiking rate recorded on the previous three inter-spike intervals. These controllers had the following forms:

$$I_{\rm stim}(t) = K_{\rm p}e(t) - K_{\rm i}\int_{t_1}^{t} R_{\rm e}(x)dx + K_{\rm base}, \qquad (5)$$

and

$$I_{\rm stim}(t) = K_{\rm p}e(t) + K_{\rm i}\int_{t_1}^{t} e(x)dx - K_{\rm i}\int_{t_1}^{t} R_{\rm e}(x)dx, \qquad (6)$$

where $K_{\rm base}$ was manually tuned.

III. RESULTS

Ziegler-Nichols method, no synaptic currents.

Using the Ziegler-Nichols method described above, we found that the output of the system started to oscillate at $K_{\mathrm{u}} = 7 \times 10^{-4}$ nA·s with the period of $P_{\mathrm{u}} = 1000$ ms. The oscillations are shown in Fig. 2. The oscillations have a regular period; however, the amplitude of the oscillations is irregular. This is not surprising given that the formula describing the system is a high-order ordinary differential equation. The Ziegler-Nichols method led to the following

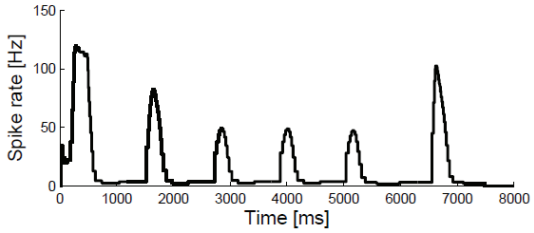

Fig. 2. Oscillations in the output of the system when using the Ziegler-Nichols method to tune gains of the PI controller.

controller gains: $K_{\mathrm{p}} = 3.15 \times 10^{-4}$ nA·s and $K_{\mathrm{i}} = 3.84 \times 10^{-7}$ nA·s. The responses of OFF and ON RGCs with synaptic blockers using these gains are illustrated in Fig. 3. A sinusoid is used as a reference signal as an example; other references may be used, i.e., the system will follow a half-wave rectified sinusoid with better accuracy in many cases. While the response of the OFF cell follows the sinusoidal reference (note large errors), the ON cell does not spike, i.e., the applied level of injected current is insufficient to bring ON cell to the spiking threshold (ON cells do not exhibit spontaneous activity when synaptic blockers are applied).

Manual tuning, no synaptic currents.

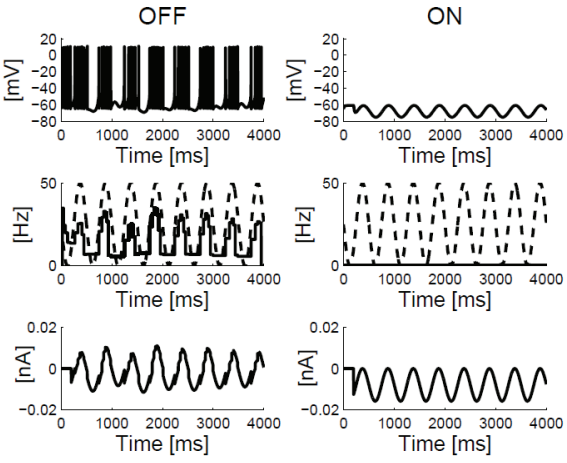

Fig. 3. Responses of OFF and ON cells with synaptic blockers using a PI controller tuned by the Ziegler-Nichols method. Left panel: OFF cell, right panel: ON cell. $K_{\mathrm{p}} = 3.15 \times 10^{-4}$ nA·], $K_{\mathrm{i}} = 3.84 \times 10^{-7}$ nA·s. Top: Membrane potential, V. Middle: Spiking rate. Dashed line: reference signal, R_{s}, solid line: output of the system, R_{e}. Bottom: Stimulation current, I_{stim}.

The results using manual tuning for OFF RGC without synaptic currents are shown in Fig. 4. Left-hand panel: the controller in the form (4), $K_{\mathrm{p}} = 3 \times 10^{-4}$ nA·s and $K_{\mathrm{i}} = 4 \times 10^{-5}$ nA·s. Right-hand panel: the controller in the form (5), $K_{\mathrm{p}} = 3 \times 10^{-4}$ nA·s and $K_{\mathrm{i}} = 1 \times 10^{-4}$ nA·s, $K_{\mathrm{base}} = 0$ nA·s. The same controller was able to work for different frequencies of the sinusoidal reference signal; results are not shown due to space constraints. These controllers were not able to bring ON cells to the spiking threshold. Note, this does not mean that it is not possible to fine-tune the controllers (4) or (5) that work for both ON and OFF RGCs. The results using the controller (5) that works

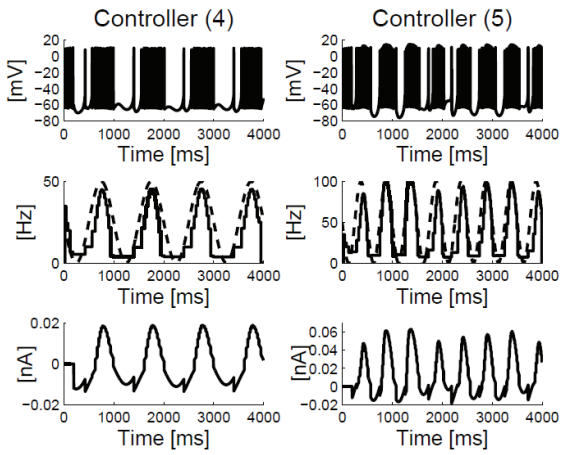

Fig. 4. Response of OFF cell with synaptic blockers using manually tuned controller. Left panel: controller (4), $K_{\mathrm{p}} = 3 \times 10^{-4}$ nA·s, $K_{\mathrm{i}} = 4 \times 10^{-5}$ nA·]. Right panel: controller (5), $K_{\mathrm{p}} = 3 \times 10^{-4}$ nA·s, $K_{\mathrm{i}} = 1 \times 10^{-4}$ nA·s, $K_{\mathrm{base}} = 0$ nA·s. Top: Membrane potential, V. Middle: Spiking rate. Dashed line: reference signal, R_{s}, solid line: output of the system, R_{e}. Bottom: Stimulation current, I_{stim}.

for both, OFF and ON cells, are shown in Fig. 5. In this case, $K_{\mathrm{p}} = 3 \times 10^{-4}$ nA·s, $K_{\mathrm{i}} = 1 \times 10^{-4}$ nA·s, $K_{\mathrm{base}} = 0.15$ nA·s. **Manual tuning, with synaptic currents.**

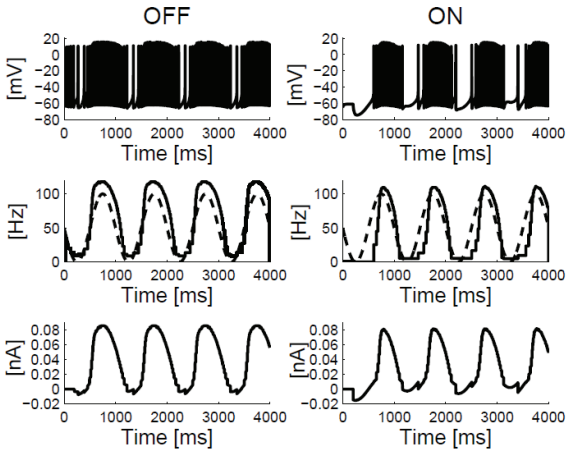

Fig. 5. Responses of OFF and ON cells with synaptic blockers using manually tuned controller (5), $K_{\mathrm{p}} = 3 \times 10^{-4}$ nA·s, $K_{\mathrm{i}} = 1 \times 10^{-4}$ nA·s, $K_{\mathrm{base}} = 0.15$ nA·s. Left panel: OFF cell, right panel: ON cell. Top: Membrane potential, V. Middle: Spiking rate. Dashed line: reference signal, R_{s}, solid line: output of the system, R_{e}. Bottom: Stimulation current, I_{stim}.

It was impossible to use the Ziegler-Nichols method to tune controller gains due to very strong intrinsic bursting at 10 Hz frequency. We found that the best controller that worked for RGCs with synaptic currents was the controller in form (6). The results for the controller (6) that works for both, OFF and ON cells with synaptic currents, are shown in Fig. 6. In this case, $K_{\mathrm{p}} = 7 \times 10^{-5}$ nA·s and $K_{\mathrm{i}} = 9 \times 10^{-5}$ nA·s. We also explored how the controller

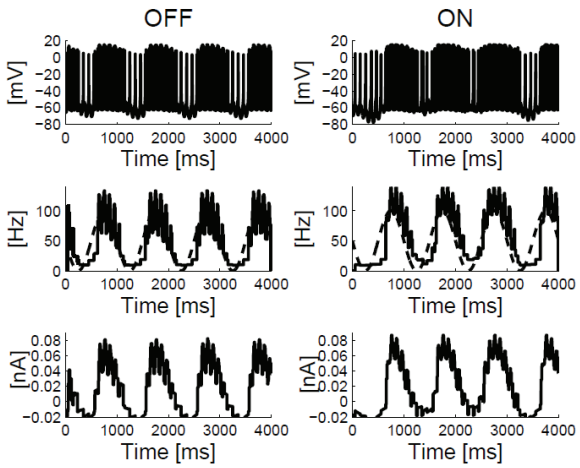

Fig. 6. Responses of OFF and ON cells with synaptic currents using manually tuned controller (6), $K_{\mathrm{p}} = 7 \times 10^{-5}$ nA·s, $K_{\mathrm{i}} = 9 \times 10^{-5}$ nA·s. Left panel: OFF cell, right panel: ON cell. Top: Membrane potential, V. Middle: Spiking rate. Dashed line: reference signal, R_{s}, solid line: output of the system, R_{e}. Bottom: Stimulation current, I_{stim}.

tuned for particular synaptic currents works during retinal degeneration. Responses of OFF and ON cells with modified synaptic currents using manually tuned controller (6), $K_{\mathrm{p}} = 7 \times 10^{-5}$ nA·s, $K_{\mathrm{i}} = 9 \times 10^{-5}$ nA·s, are shown in Fig. 7. In this case, the conductance of excitatory current in OFF and ON cells was multiplied by 0.8, which roughly corresponds to 20% decrease in excitatory synapses, while the gains of the controller were left unchanged.

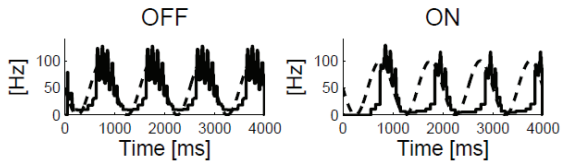

Fig. 7. Responses of OFF and ON cells with modified synaptic currents using manually tuned controller (6), $K_{\mathrm{p}} = 7 \times 10^{-5}$ nA·s, $K_{\mathrm{i}} = 9 \times 10^{-5}$ nA·s. Left panel: OFF cell, right panel: ON cell. Dashed line: reference signal, R_{s}, solid line: output of the system, R_{e}. g_{exc} is reduced by 20% in both OFF and ON RGCs.

IV. Conclusions

This paper shows preliminary modelling results of a stimulation strategy that can be used to adjust stimulation current in a visual prosthetic device. Single-compartment Hodgkin-Huxley-type models were used to investigate responses of ON and OFF ganglion cells to electrical stimulation using a closed-loop paradigm.

The results presented here were obtained under several assumptions that need to be relaxed in the future. In particular, a neural population response to electrical stimulation has to be considered. Various controller designs need to be considered. The modelling results show that a standard PID controller is not the best choice to use in a neuroprosthetic device. More advanced controllers that account for stimulus and output constraints and system's nonlinearities, such as model-predictive controllers, deserve future considerations.

Usually, electrical stimuli in a clinical device are brief ($<$ 800ms) biphasic pulses. This is different to what is proposed here. The issue of the charge balanced brief biphasic pulses, should be addressed in the future.

Acknowledgments

This research was supported by the Australian Research Council (DE120102210). The Bionics Institute acknowledges the support it receives from the Victorian Government through its Operational Infrastructure Support Program. This research was supported by the Australian Research Council through its Special Research Initiative in Bionic Vision Science and Technology grant to Bionic Vision Australia.

References

[1] A.K. Ahuja, J.D. Dorn, A. Caspi, M.J. McMahon, G. Dagnelie, L. daCruz, P. Stanga, M.S. Humayun, R.J. Greenberg. Blind subjects implanted with the Argus II retinal prosthesis are able to improve performance in a spatial-motor task. *Br. J. Ophthalmol.,* 95(4): 539 - 543, 2010.

[2] J. F. Fohlmeister and R. F. Miller. Impulse encoding menchanisms of ganglion cells in the tiger salamander retina. *J. Neurophysiol.,* 78: 1935-1947, 1997.

[3] M. Hines. NEURON a program for simulation of nerve equations. *In: Neural Systems: Analysis and Modeling, edited by F. Eckman. Norwell, MA: Kluwer Academic Publishers*, 1993.

[4] T. Kameneva, H. Meffin, A.N. Burkitt. Modelling intrinsic electrophysiological properties of ON and OFF retinal ganglion cells. *J. Comput. Neurosci.,* 31(3), 547 - 561, 2011.

[5] T. Kameneva, D. B. Grayden, H. Meffin, A. N. Burkitt. Simulating electrical stimulation of degenerative retinal ganglion cells with biphasic pulse trains. *Proc. of the the EMBS conference,* 7103 - 7106, 2011.

[6] R. Margalit et al. Retinal prosthesis for the blind. *Survey Ophtalm.,* 47(4): 335 - 356, 2002.

[7] D.J. Margolis, P.B. Detwiler.Different mechanisms generate maintained activity in ON and OFF retinal ganglion cells. *J. Neurosci.*, 27(22): 5994-6005, 2007.

[8] D.J. Margolis, G. Newkirk, T. Euler, P.B. Detwiler. Functional stability of retinal ganglion cells after degeneration-induced changes in synaptic input. *J. Neurosci.,* 28: 6526-6536, 2008.

[9] O. Miranda-Dominguez, J. Gonia, T.I. Netoff. Firing rate control of a neuron using a linear proportional-integral controller. *J. Neural Eng.,* 7(6): 066004, 2010.

[10] D.J. Mogul, Y. Li, M.E. Colpan. Using electrical stimulation and control feedback to modulate seizure activity in rat hippocampus, *Proc. AES/ACNS Conf.,* 46: 331, 2005.

[11] R.D. Traub, E.H. Buhl, T. Gloveli, M.A. Whittington. Fast Rhythmic Bursting Can Be Induced in Layer 2/3 Cortical Neurons by Enhancing Persistent NaP Conductance or by Blocking BK Channels. *J. Neurophysiol.*, 89: 909-921, 2003

[12] A. Wallach, D. Eytan, A. Gal, C. Zrenner, S. Marom. Neuronal response clamp. *Front. Neuroeng.,* 4: 1 - 10, 2011.

[13] X.-J. Wang, J. Rinzel, M. Rogawski. A model of the T-type calcium current and the low-threshold spike in thalamic neurons. *J. Neurophysiol.,* 66: 839-850, 1991.

[14] I. van Welie, M. W. H. Remme, J. van Hooft, W. J. Wadman. Different levels of Ih determine distinct temporal integration in bursting and regular-spiking neurons in rat subiculum. *J. Physiol.,* 576.1: 203-214, 2006.